

COMPUTATIONAL ANALYSIS OF THE INFLUENCE OF THERMAL AND GEOMETRICAL PARAMETERS ON POLLUTANT DISPERSION IN STREET CANYON

Janaina Ferreira Batista Leal, janaina@debas.eel.usp.br

Escola de Engenharia de Lorena da Universidade de São Paulo
Rodovia Lorena-Itajubá, Km 74.5, Lorena – SP 12600-970

Jurandir Itizo Yanagihara, jiv@usp.br

Escola Politécnica da Universidade de São Paulo
Av. Prof. Mello Moraes 2231, São Paulo – SP 05586-060

Abstract. *The dispersion of air pollutants in large metropolitan areas is related to the wind flow around the street canyons. Numerical studies have been carried out in order to ascertain what are the parameters that influence the wind flow and the pollutant dispersion in a street canyon. Some of these parameters are related to thermal effects which promote an upsurge of a strong buoyancy flow close to the heating surfaces, leading to a combined thermally and mechanically induced flow which affects the flow fields and the pollutant dispersion. In the present study a finite-volume commercial code (FLUENT) was used for the numerical simulation of the flow field. The modeling of the conservation equations is based on Reynolds Averaged Navier-Stokes (RANS) and uses the standard $k-\varepsilon$ turbulence model. For this study, it is considered the heating of building surfaces and street canyon bottom surface for different aspect ratios (building height per street width). An additional parameter was included, namely the temperature difference between the street canyon surfaces and the free-stream air. Another important parameter that was analyzed is the location of the pollution source, ranging from the centre of the street canyon to positions close to the leeward building, that is, the upwind side of the canyon, and the windward building, the downwind side of the canyon. The results provide important information about the influence of such parameters on pollutant dispersion.*

Keywords: *street canyon, pollutant dispersion, thermal effects*

1. INTRODUCTION

The traffic of vehicles in urban areas is the main reason of the atmospheric pollution due to its emission of gases and particulates. The so-called street canyons are examples these sites, formed along a street in a densely built urban area with buildings on both sides, where there is high pollutant concentration. As these pollutants are harmful to the human health, it is important to develop models that can predict pollution levels in these environments, aiming the preservation of the air quality standard.

Several models have been developed to study the parameters that influence the pollutant dispersion process in street canyons such as geometry of the building (height, width and roof shape), street dimensions (breadth and width), environmental conditions (wind velocity and direction), thermal stratification (thermal isolation and orientation of the sun, building and street thermal capacity), plume buoyancy, vegetation or landscape and surface roughness, movement of vehicles (size, number and frequency), among others (Meroney *et al.*, 1996; Gerdes and Olivari, 1999; Sagrado *et al.*, 2002).

The aspect ratio is one of the geometric parameters that has great influence on the flow field in an urban street canyon and is defined as the ratio of the building height to the width between buildings. Two-dimensional numerical models varying the aspect ratio were developed by several researchers such as Sini *et al.* (1996); Leitl and Meroney (1997); Baik and Kim (1999); Assimakopoulos *et al.* (2003); Chan *et al.* (2002); Nazridoust and Ahmadi (2006). They used the Standard $k-\varepsilon$ turbulence model and its variations based on Reynolds-Averaged Navier-Stokes (RANS) flow equations to solve the flow field and observed that the number of vortices increases with the increase of aspect ratio.

The effects on the airflow of heated building or street surfaces have also a great importance in determining flow pattern and pollutant dispersion in street canyons. Some researchers such as Kim and Baik (1999, 2001), Louka *et al.* (2002), Xie *et al.* (2005b), Moussiopoulos *et al.* (2005), Tsai *et al.* (2005) and Xie *et al.* (2006, 2007) developed thermal studies for different aspect ratios and different heating intensities. Assimakopoulos *et al.* (2003) showed results about the effects on the dispersion patterns when the location of the pollution source is altered, e.g., in the center of canyon, close to upwind building and close to downwind building.

Leal and Yanagihara (2008) showed results for different aspect ratios considering isothermal and non-isothermal conditions and the authors concluded that street canyons with tall buildings should be avoided in city planning, due to its direct impact on the drivers, bicyclists, motorcyclist, pedestrians, people working nearby, and vehicle passengers.

This present work is a continuation of this early study and shows with more details the thermal effects on the pollutant dispersion for two aspect ratios, and presents the concentrations fields to different temperature gradients with bottom heating of a street canyon and the effects of altering the source pollutant location.

2. NUMERICAL MODEL

The numerical model used in this study is the same of the previous study (Leal and Yanagihara, 2008) considering thermal effects. The finite volume method was used to model the governing equations for fluid flow and pollutant dispersion. The standard $k-\varepsilon$ turbulence model is adopted, which is based on Reynolds Averaged Navier-Stokes (RANS) flow equations. The flow is considered two-dimensional, steady and incompressible. In the case with thermal effects, the density is a function of temperature for incompressible turbulent inert flow and the air density changes due to the increase of air temperature. The buoyancy forces induce the air motion and these forces are added in the momentum conservation equation. Adopting the Boussinesq approximation, it is assumed that the specific mass and the other physical parameters do not change except for the specific mass in the buoyancy forces term. The mass and momentum conservation equations follow

$$\frac{\partial U_i}{\partial x_i} = 0 \quad (1)$$

$$\frac{\partial}{\partial x_j} (U_i U_j) = \left(\frac{\rho - \rho_n}{\rho_n} \right) g_i - \frac{1}{\rho} \frac{\partial P}{\partial x_i} + \frac{\partial}{\partial x_j} \left(\nu \frac{\partial U_i}{\partial x_j} \right) + \frac{\partial}{\partial x_j} (-\overline{u'_i u'_j}) \quad (2)$$

where U is the mean velocity, u' is the velocity fluctuation, P is the mean pressure and ν is the kinematic viscosity, g_i is the component of the gravitational acceleration, ρ is the fluid specific mass and ρ_n is the reference specific mass.

The specific mass deviation $\rho - \rho_n$ is related to the temperature through the following linear equation of state:

$$\frac{\rho - \rho_n}{\rho_n} = -\beta (\Theta - \Theta_n) \quad (3)$$

where Θ is the mean temperature and β is thermal expansion coefficient.

The momentum equations include turbulent fluxes $-\overline{u'_i u'_j}$ which are modeled using the Boussinesq hypothesis so that Reynolds stresses can be linked to the mean rates of deformation. This term is modeled as

$$-\overline{u'_i u'_j} = \nu_t \left(\frac{\partial U_i}{\partial x_j} + \frac{\partial U_j}{\partial x_i} \right) - \frac{2}{3} k \delta_{ij} \quad \delta_{ij} = \begin{cases} 1 & \text{for } i = j \\ 0 & \text{for } i \neq j \end{cases} \quad (4)$$

where ν_t is the eddy viscosity (or turbulent viscosity), k the kinetic energy and δ_{ij} the Kronecker delta. The eddy viscosity ν_t is related to the turbulent kinetic energy k and its rate of dissipation ε and is modeled as $\nu_t = C_\mu k^2 / \varepsilon$.

The energy equation, takes into account the thermal effects, allowing the calculation of the temperature field.

$$\frac{\partial (U_i \Theta)}{\partial x_i} = \frac{\partial}{\partial x_i} \left(K_t \frac{\partial \Theta}{\partial x_i} \right) \quad (5)$$

The species (pollutants) transport equation is

$$\frac{\partial}{\partial x_i} (U_i C) = \frac{\partial}{\partial x_i} \left(\frac{\nu_t}{S_{ct}} \frac{\partial C}{\partial x_i} \right) \quad (6)$$

where C is the mean concentration. In this equation the molecular diffusion term is ignored since the turbulent diffusion term is predominant and S_{ct} is the turbulent Schmidt number.

Two additional conservation equations must be solved: one for the turbulent kinetic energy k and other for its rate of dissipation ε . The turbulence production due to the buoyancy effect is included in the momentum transport modeling.

$$\frac{\partial}{\partial x_i} (U_i k) = \frac{\partial}{\partial x_i} \left[\left(\nu + \frac{\nu_t}{\sigma_k} \right) \frac{\partial k}{\partial x_i} \right] + P_k - \varepsilon - \beta g_i u'_i \overline{\theta'} \quad (7)$$

$$\frac{\partial}{\partial x_i}(U_i \varepsilon) = \frac{\partial}{\partial x_i} \left[\left(\nu + \frac{\nu_t}{\sigma_\varepsilon} \right) \frac{\partial \varepsilon}{\partial x_i} \right] + C_{1\varepsilon} \frac{\varepsilon}{k} \left(P_k - \beta g_i \overline{u_i \theta'} \right) - C_{2\varepsilon} \frac{\varepsilon^2}{k} \quad (8)$$

$$-\overline{u_i \theta'} = K_t \frac{\partial \Theta}{\partial x_i} \quad (9)$$

where $\overline{u_i \theta'}$ is the turbulent heat flux, K_t is the turbulent diffusivity coefficient, ($K_t = \nu_t / Pr_t$), where Pr_t is the turbulent Prandtl number. P_k is the rate of production of kinetic energy, and σ_k , σ_ε , $C_{1\varepsilon}$ and $C_{2\varepsilon}$ are constants of the standard k - ε model. The rate of production of turbulent kinetic energy is calculated by Eq. (10).

$$P_k = \nu_t \frac{\partial U_i}{\partial x_j} \left(\frac{\partial U_i}{\partial x_j} + \frac{\partial U_j}{\partial x_i} \right) \quad (10)$$

The constants used in equations above are specified as (Sini *et al.* 1996):

$$C_\mu = 0.09 \quad C_{1\varepsilon} = 1.44 \quad C_{2\varepsilon} = 1.92 \quad \sigma_k = 1.0 \quad \sigma_\varepsilon = 1.3 \quad Sc_t = 0.9 \quad Pr_t = 0.7$$

The above governing equations set is solved numerically on a staggered grid system using the finite-volume method following the Semi-Implicit Method for Pressure-Linked Equation (SIMPLE) algorithm described by Patankar (1980). The 2nd order upwind scheme was used for the modeling of the convection-diffusion coupling. All the above calculations were performed using the FLUENT code. The effects of the street aspect ratio on the flow field and pollutant distribution in urban street canyons for the isothermal and no-isothermal cases are investigated considering two different aspect ratios. In order to examine the influence of thermal effects the following cases are considered: no heating, heating of leeward side of building, heating of windward side of building and heating of bottom of street canyon.

The case of bottom heating is investigated for three different temperature gradients, $\Delta\Theta = 5$ K, 8 K and 10 K, where $\Delta\Theta$ is the temperature difference between the street canyon surfaces and the air ambient. Figure 1 shows the model domain configuration where the domain size is 100 m in horizontal direction and 160 m in vertical direction, and the grid interval is 1.25 m in both directions. The street canyon width is 40 m. Building heights of 40 m and 80 m were considered, with aspect ratios of 1.0 and 2.0, respectively. The initial conditions for wind velocities, turbulent kinetic energy and its dissipation, and air temperature are specified as

$$U_0 = 2.5 \left(\frac{z}{z_r} \right)^{0.299} \quad W_0 = 0 \quad k_0 = 0.003 U_0^2 \quad \varepsilon_0 = \left(C_\mu^{3/4} k_0^{3/2} \right) / \kappa z \quad \Theta_0 = 293K$$

where $z_r = 10$ m is the reference height in meters and $\kappa = 0.4$ is the von Kármán constant. Initially, the shear layer given by profile is assumed to exist up to $z = 10$ m above the building roof level and above it the velocity is assumed to be constant. No-slip boundary conditions are applied at the ground and building surfaces. At the outflow and upper boundaries, the gradient of any variable is set to zero.

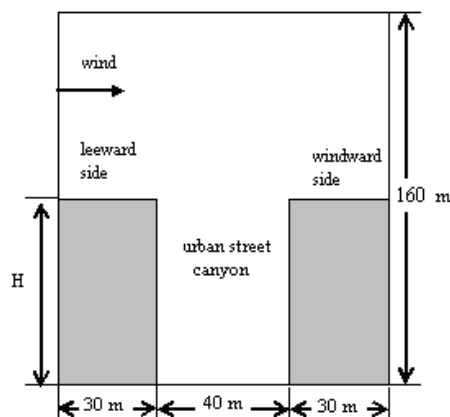


Figure 1. Sketch of the calculation domain

3. RESULTS AND DISCUSSION

The thermal effects on the flow fields in urban street canyons with different aspect ratios are investigated for the cases of upwind building-wall heating, street-canyon bottom heating, and downwind building-wall heating for two aspect ratios. Figure 2 shows the flow fields and concentration distribution in a regular urban street canyon with an aspect ratio of 1 in the cases of upwind building-wall heating and downwind building-wall heating with $\Delta\Theta = 5$ K, that is, temperature difference between the street canyon surfaces and the air ambient. For the study of pollutant distribution it is considered the case of street-level emission source, which can be regarded as representing the case of pollutant emission from motor vehicles. The pollutant considered is carbon monoxide, which is relatively stable, easily measured and comes mainly from vehicle emissions. In this case there is 32 emission points at a rate of 5 ppbs^{-1} in each grid point that is equivalent to a total emission of 160 ppbs^{-1} .

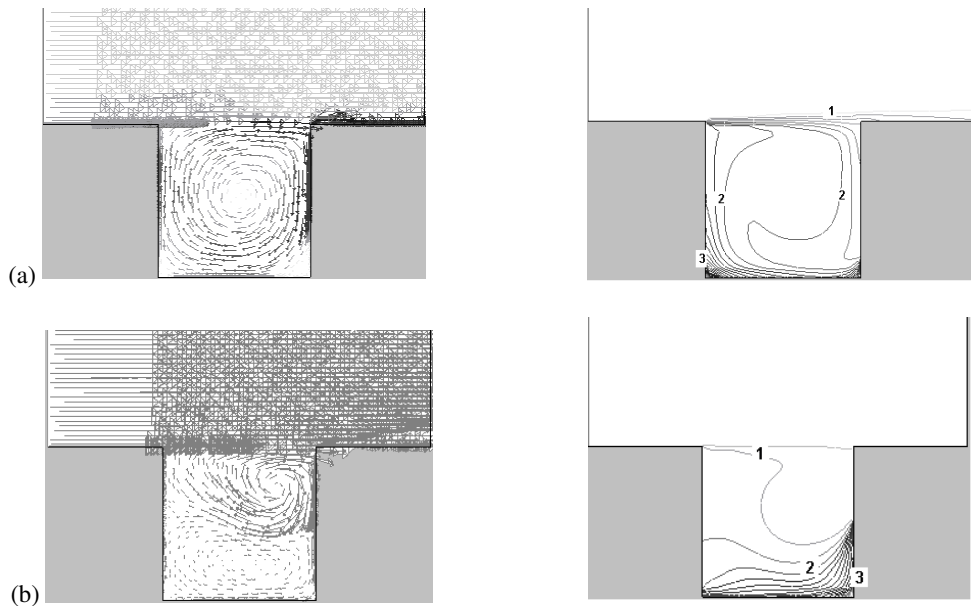


Figure 2. Wind fields and concentration profile for an aspect ratio of 1 ($\Delta\Theta = 5$ K) in the cases of (a) leeward side heating and (b) windward side heating.

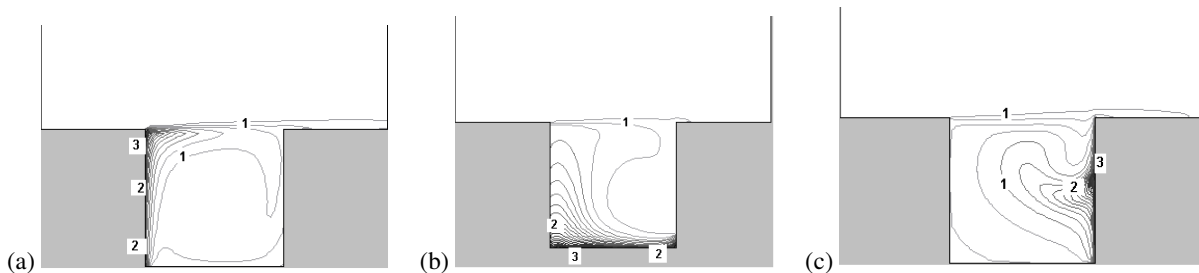


Figure 3. Temperature fields for an aspect ratio of 1 in the cases of (a) leeward side heating, (b) bottom heating, and (c) windward side heating.

In the case of no heating, leeward side heating and bottom heating the wind fields and concentration profile are similar. In the case of leeward heating can be observed from Fig.3 (a) that there is a large horizontal temperature gradient near the upwind building, inducing an upward motion on the upwind side. The clockwise vortex that is mechanically induced by the ambient wind is strengthened by this thermal upward motion and one vortex appears as well. Analyzing the pollutant concentration fields we observed that the concentration distribution is controlled mainly by the vortex circulation. Near the windward building the concentration is low at any height, while near the leeward side of building the concentration is high at any height, as a result of the advection and diffusion processes. In the case with bottom heating, there is also one vortex, although there is the upsurge of a vertical temperature gradient near the street canyon bottom as observed from Fig. 3 (b). The vortex produces a horizontal motion in the lower layer that shifts the maximum temperature axis toward the leeward building. This induces a thermal upward motion which strengthens the vortex and enhances the upward motion mechanically induced by the ambient wind. In the case of windward heating

shown by Fig. 3 (c), the horizontal temperature gradient is large near the windward building. The upsurge of a upward buoyancy flux opposes the downward advection flux along the wall, weakening the original vortex and producing the split the flow structure into two counter-rotating vortices: a clockwise top vortex and a reverse vortex within the canyon. This flow structure accumulates the pollutants at the bottom of the canyon and mainly at the windward side of the building until a certain height.

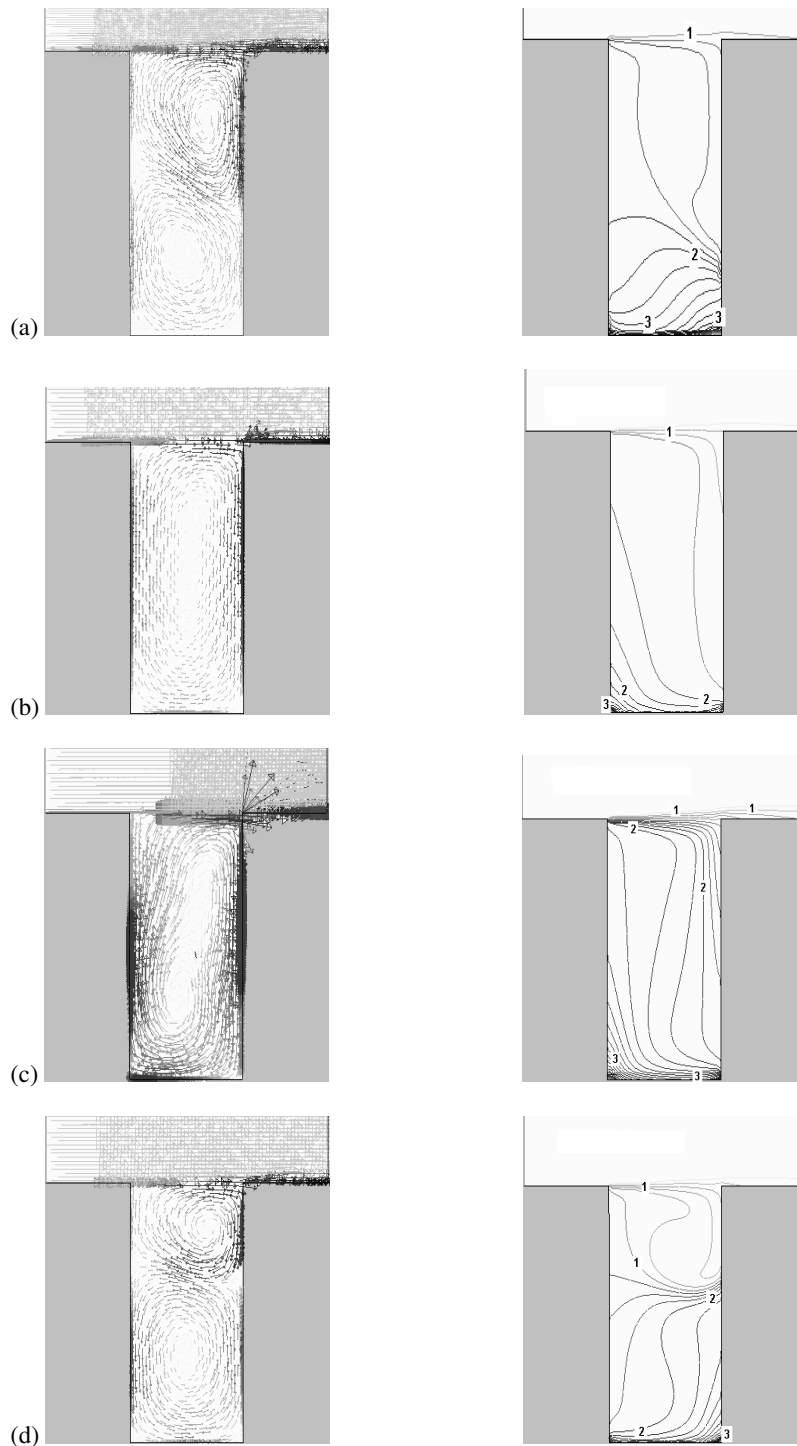


Figure 4. Wind fields and concentration profile for an aspect ratio of 2 ($\Delta\Theta = 5$ K) in the cases of (a) no heating, (b) leeward side heating, (c) bottom heating, and (d) windward side heating.

For the aspect ratio of 2.0, two counter-rotating vortices are formed as can be seen from Fig. 4 (a) and there are two different pattern of the concentration distribution in the lower and upper regions. In spite of the difference between these regions, there is a common feature: in the regions of the upward motion there are high pollutant concentrations, that is, on the windward side of the lower region and the leeward side of the upper region. In the regions of the downward motion there are low pollutant concentrations. This feature is directly linked to the two counter-rotating vortices circulation. Highly polluted air passing through the street-level source is advected upward on the windward side of the lower region. The pollutant concentration in this region is high, with the concentration decreasing with height.

Figure 4 (b) shows the case of leeward side heating where the thermal upward motion near the leeward side is weakened in the lower region, due to the mechanical downward motion in this region. On the other hand, in the upper region, the flow is strengthened due to the mechanical upward motion in the region and, as a result, one vortex is generated in the street canyon. In this case, the transport mechanism of pollutants is similar to that corresponding to an aspect ratio of 1.0, characteristic of a one vortex circulation as shown by the pattern of the temperature field (Fig. 5 (a)).

Figure 4 (c) presents the wind fields and concentration profile for the case of bottom heating, and in the Fig. 5 (b) it can be seen that there are higher temperatures near the leeward building, that induces the upward motion in this side, weakening the lower vortex and strengthening the upper vortex, producing one vortex. The concentration distribution is similar to that corresponding to an aspect ratio of 1.0 and thus, the transport mechanism of pollutants is also similar, characteristic of vortex circulation.

Figure 4 (d) presents the windward side heating case, where there is the upsurge of two counter-rotating vortices as in the no heating case, due to the thermal upward motion near the windard building that strengthens the lower vortex and weakens the upper vortex. The counter-clockwise lower vortex has a strong intensity, transporting the pollutants to the windward side. Figure 5 (c) shows the temperature fields for this case.

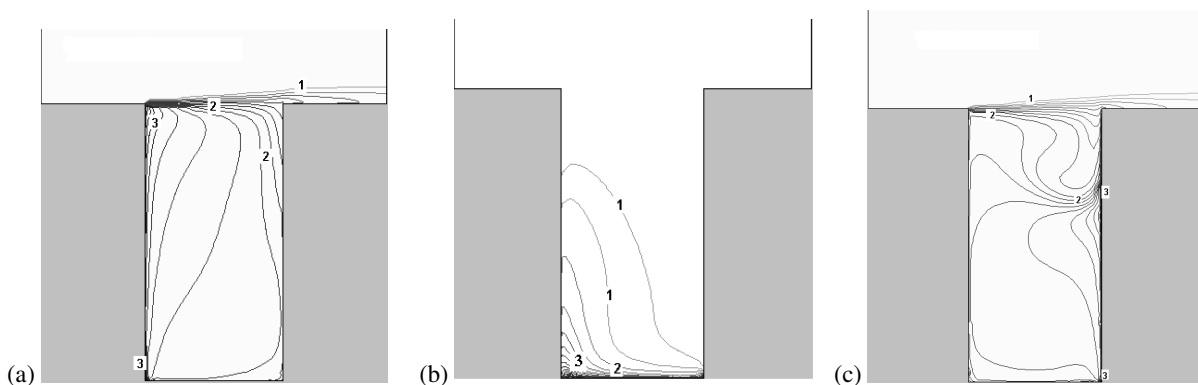


Figure 5. Temperature fields for an aspect ratio of 2 in the cases of (a) leeward side heating, (b) bottom heating, and (c) windward side heating.

Figure 6 shows the temperature fields considering the case of bottom heating to a temperature difference of 5 K, 8 K and 10 K in the case of the aspect ratio of 1. In all cases there is only one vortex. The cases of temperature difference of 8 K and 10 K are similar to the case with temperature difference of 5K. In this case there is a vertical temperature gradient near the bottom of the street canyon and the larger temperatures are located near the leeward building that produces a thermal upward motion which strengthens the vortex and enhances the upward motion mechanically induced by the ambient wind, producing one vortex.

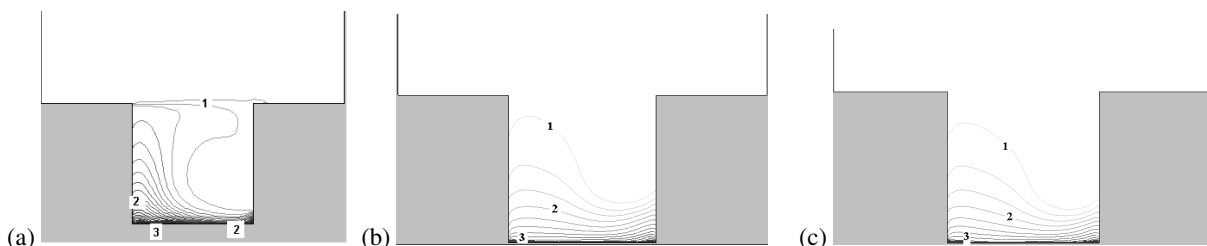


Figure 6. Temperature fields for an aspect ratio of 1 with bottom heating and temperature differences of (a) 5 K, b) 8 K and c) 10 K.

Figure 7 shows the wind fields and temperature fields considering the case of bottom heating to a temperature difference of 5 K, 8 K and 10 K in the case of the aspect ratio of 2. It can be seen that the position of the maximum

temperature is close to the leeward building, similarly to the case of temperature difference of 5K. In the case of no heating, there are two counter-rotating vortices. For temperature differences of 8 K and 10 K, there is a strong upward motion near the leeward building that removes the lower vortex. Therefore the upper vortex that is mechanically generated starts to merge into the lower layer vortex but this process remains incomplete. Two clockwise rotating vortices are generated in the vertical direction and between the vortices upsurges a saddle point.

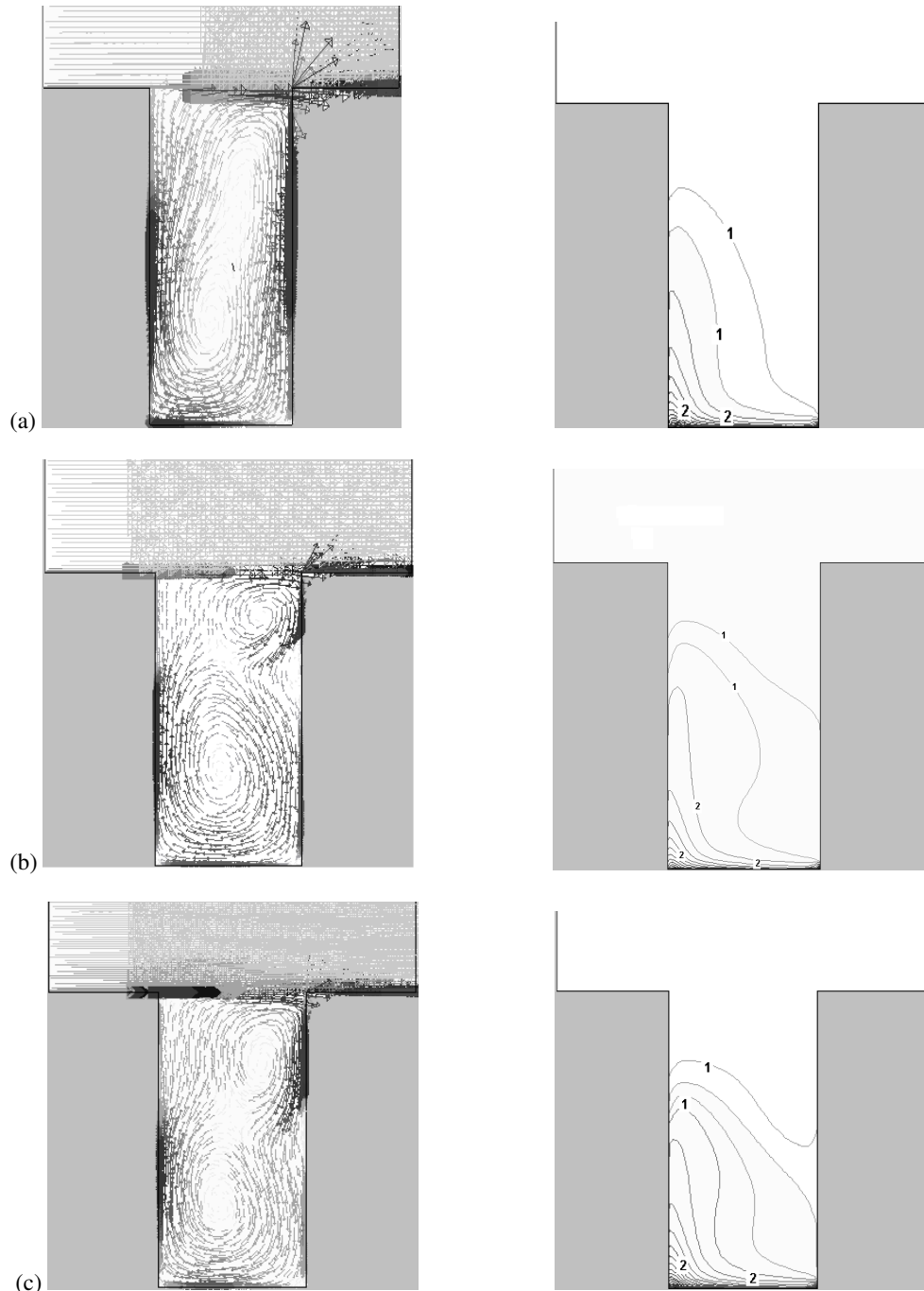


Figure 7. Wind fields and temperature fields for an aspect ratio of 2 with bottom heating and temperature differences of (a) 5 K, (b) 8 K and (c) 10 K.

The altering of the location of the pollution source to two different aspect ratios and the effect on the pollutant dispersion in the isothermal case is showed in Fig. 8 e Fig. 9, with carbon monoxide as the pollutant considered. The source length is equal to 16 meters and the pollution source is located (a) at street level, (b) in the centre of the street, (c) close to the leeward building and (d) close to the windward building.

Figure 8 (a) shows the concentration distribution for the case of aspect ratio of 1 when the pollution source is located at street level which can be regarded as representing the case of pollutants emission from motor vehicles. In this case there are 32 emission points at a rate of 5 ppbs^{-1} in each grid point that is equivalent to total emission of 160 ppbs^{-1} . In this case there is only one clockwise vortex and a low-concentration region can be verified near the windward side of building, where a strong downward motion exists. In this side, the ambient air with relatively low concentration enters the street canyon by the downward vortex circulation. At leeward side there is high concentration at any height of the street canyon, where a strong upward motion exists, and the concentration decreases from the floor to the roof of the upstream building. In this side, highly polluted air passing through the street-level is advected upward on the leeward side.

Figure 8 (b) shows the case where the pollution source is in the centre of the street and it can be seen a region of low concentration at any height of the street canyon near the windward side of building, where a strong downward motion exists due to vortex. A region of high concentration is located near the leeward building.

In the case of Fig. 8 (c) the pollution source is located near the leeward building, and the pollutants concentration is lower close to the windward building and higher close to the leeward building.

Figure 8 (d) shows the case when the pollution source is located near the windward and it can be seen that the pollutants disperse better than for the other cases.

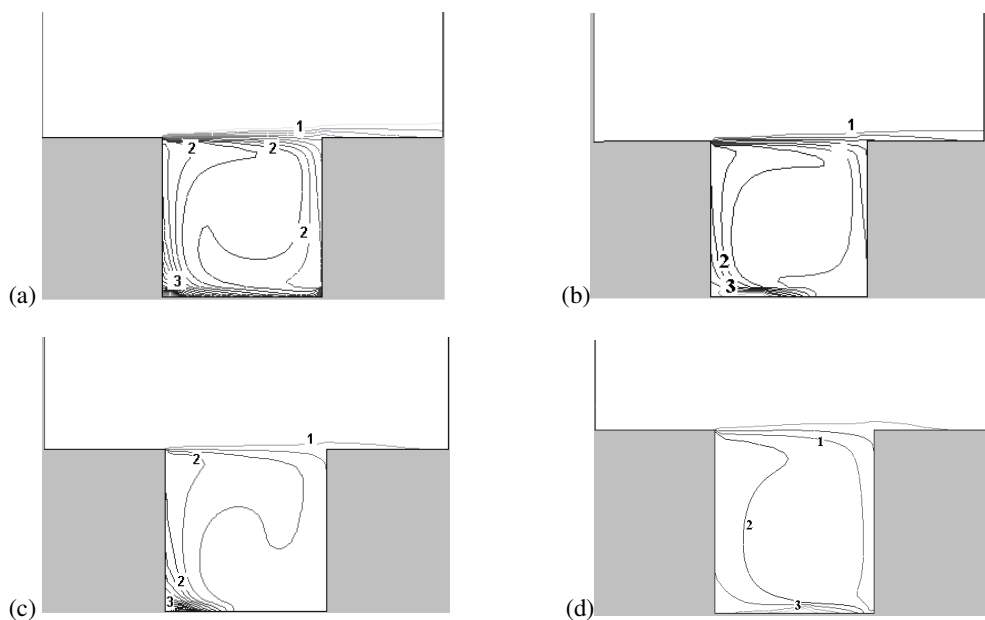


Figure 8. Concentration profiles for aspect ratio of 1 for pollution source (a) at level of the street, (b) in the centre of the street, (c) close to the leeward building and (d) close to the windward building.

Figure 9 (a) shows the concentration distribution for the case of aspect ratio of 2 when the pollution source is located at street level and it can be seen that there are two different pattern of the concentration distribution in the lower and upper regions. In spite of the difference between these regions, there is a common feature: in the regions of the upward motion there are high pollutant concentrations, that is, on the windward side of the lower region and the leeward side of the upper region. In the regions of the downward motion there are low pollutant concentrations. This feature is directly linked to the two counter-rotating vortices circulation. Highly polluted air passing through the street-level source is advected upward on the windward side of the lower region. The pollutant concentration in this region is high, with the concentration decreasing with height. Figure 9 (b) shows the case where the pollution source is in the centre of the street. The concentration distribution is similar to the case with pollution source at street level where there are two different pattern of the concentration distribution in the lower and upper regions directly linked to the two counter-rotating vortices circulation. High pollutant concentration is encountered on the leeward side of the upper region and on the windward side of the lower region, from the line source. In the case of Fig. 9 (c) the pollution source is located near the leeward building. The pollutants disperse more in the lower layer due to counter-clockwise vortex that upsurges in this lower region. Figure 9 (d) shows the case when the pollution source is located near the windward and pollutant concentration follows the vortices circulation as mentioned.

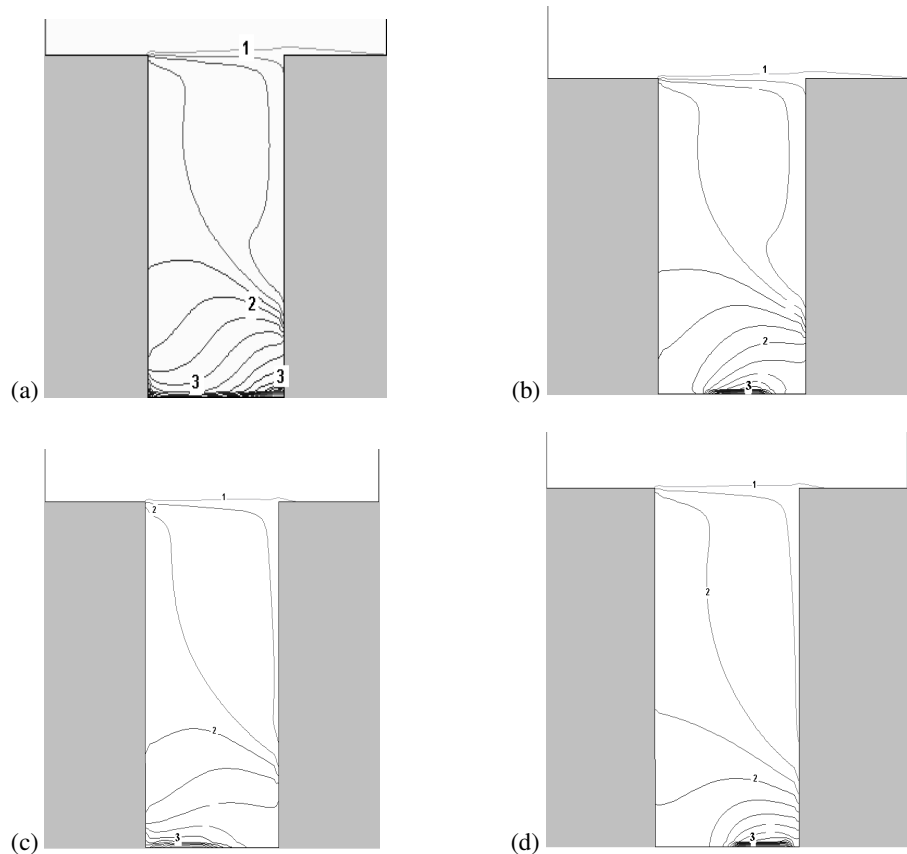


Figure 9. Concentration profiles for aspect ratio of 2 for pollution source (a) at level of the street, (b) in the centre of the street, (c) close to the leeward building and (d) close to the windward building.

4. CONCLUSIONS

In early studies the authors showed that the thermal effects have a great influence on the flow patterns and pollutants dispersion. In this work this topic is addressed with more details in the cases of no heating, leeward side heating, bottom heating and windward side heating for a street canyon with aspect ratio of 1 and 2. For aspect ratio of 1 for the cases of no heating, leeward side heating and bottom heating for a temperature gradient of $\Delta\Theta = 5$ K, it was observed the upsurge of only one vortex and a low-concentration region near the windward side and a high concentration at leeward side, where the concentration decreases from the floor to the roof of the upstream building. The case of windward side heating presented two counter-rotating vortices with higher concentrations in the windward side. For the case of aspect ratio of 2 with leeward side heating and bottom heating, it was observed only one vortex, because of larger temperatures close to the leeward building that induce the upward motion in this side. This motion weakens the lower vortex and strengthens the upper vortex that appears in the case of no heating, producing one vortex with the corresponding concentration profile. For windward side heating, there are two counter-rotating vortices as in the no heating case, due to the thermal upward motion near the windward building. This strengthens the lower vortex and weakens the upper vortex, causing higher concentrations in the windward side of the lower region and in the leeward side of the upper region. In the case of bottom heating it was studied also the effect of changing of the temperature gradient from $\Delta\Theta = 5$ K to 8 K and 10 K on the velocity fields for street canyons with aspect ratios of 1 and 2. For aspect ratio of 1, the changes were not significant, with the production of only one vortex. According to Kim and Baik (2001) this result is reasonable for relatively small aspect ratios. For aspect ratio of 2, the increasing of the temperature gradient (8 K and 10 K) produces a strong upward motion near the leeward building that removes the lower vortex and generates two combined clockwise co-rotating vortices. This result is observed when there is the increasing of the heating intensity according to Kim and Baik (2001). The altering of the location of the pollution source for aspect ratios of 1 and 2 and the effect on the pollutant dispersion in the isothermal case was studied considering the pollution source at street level, in the centre of the street, near the leeward building and near the windward building. For aspect ratio of 1 and with the pollutant source positioned at street level, in the centre of the street and close to the leeward building, the concentration profiles were similar, with higher concentrations near the upwind building and lower close the windward building. In the case in which the pollution source is located near the windward building, it was observed that the pollutants disperse better than for the other cases. For aspect ratio of 2 for the positions at street level, in the centre of the street and close to

windward building, it is observed higher concentrations in the windward side of the lower region and the leeward side of the upper region. This feature is directly linked to the two counter-rotating vortices circulation. In the case where the pollution source is close to the leeward building the pollutants disperse more in the lower layer due to counter-clockwise vortex that upsurges in this lower region. The results presented in this work showed the great influence of thermal aspects, due to strong buoyancy flow that upsurges close to the heating surfaces, leading to a combined thermally and mechanically induced flow affecting the flow field and the pollutant dispersion in the street canyons. The changing of the temperature gradient in the case of street canyon bottom heating affected more the results for aspect ratio of 2.

5. ACKNOWLEDGEMENTS

The authors are grateful for the support provided by FAPESP.

6. REFERENCES

- Assimakopoulos, V.D., ApSimon, H.M. and Moussiopoulos, N., 2003, "A Numerical Study of Atmospheric Pollutant Dispersion in Different Two-Dimensional Street Canyon Configurations", *Atmospheric Environment*, Vol. 37, pp. 4037-4049.
- Baik, J.J. and Kim, J.J., 1999, "A Numerical Study of Flow and Pollutant Dispersion Characteristics in Urban Street Canyons", *Journal of Applied Meteorology*, Vol. 38, pp. 1576-1589.
- Chan, T.L., Dong, G., Leung, C.W., Cheung, C.S. and Hung, W.T., 2002, "Validation of a Two-Dimensional Pollutant Dispersion Model in an Isolated Street Canyon", *Atmospheric Environment*, Vol. 36, pp. 861-872.
- Gerdes, F. and Olivari, D., 1999, "Analysis of Pollutant Dispersion in an Urban Street Canyon", *Journal of Wind Engineering and Industrial Aerodynamics*, Vol. 82, pp. 105-124.
- Kim, J.J. and Baik, J.J., 1999, "A Numerical Study of Thermal Effects on Flow and Pollutant Dispersion in Urban Street Canyons", *Journal of Applied Meteorology*, Vol.38, pp. 1249-1261.
- Kim, J.J. and Baik, J.J., 2001, "Urban Street Canyon Flows with Bottom Heating", *Atmospheric Environment*, Vol. 35, pp. 3395-3404.
- Leal, J.F.B. and Yanagihara, J.I., 2008, "Computational Analysis of Thermal Effects on Flow and Pollutant Dispersion in Street Canyon", *Proceedings of the 12th Brazilian Congress of Thermal Engineering and Sciences*, Curitiba, Brazil, code 3_4973.
- Leitl, B.M. and Meroney, R.N., 1997, "Car Exhaust Dispersion in a Street Canyon. Numerical Critique of a Wind Tunnel Experiment", *Journal of Wind Engineering and Industrial Aerodynamics*, pp. 293-304.
- Louka, P., Vachon, G., Sini, J.F., Mestayer, P.G., Rosant, J.M., 2002, "Thermal Effects on the Airflow in a Street Canyon – NANTES'99 Experimental Results and Model Simulations", *Water, Air, and Soil Pollution: Focus 2*, pp. 351-364.
- Meroney, R.N., Pavageau, M., Rafailidis, S. and Schatzmann, M., 1996, "Study of Line Source Characteristics for 2D Physical Modeling of Pollutant Dispersion in Street Canyons", *Journal of Wind Engineering and Industrial Aerodynamics*, Vol. 62, pp. 37-56.
- Moussiopoulos, N., Ossanlis, I. and Barmpas, P., 2005, "A Study of Heat Transfer Effects on Air Pollution Dispersion in Street Canyons by Numerical Simulations", *Inter. J. of Environment and Pollution*, Vol. 25, pp.131-144.
- Nazridoust, K. and Ahmadi G., 2006 "Airflow and Pollutant Transport in Street Canyons", *Journal of Wind Engineering and Industrial Aerodynamics*, Vol. 94, pp.491-522.
- Sagrado, A.P.G., van Beeck, J., Rambaud, P. and Olivari, D., 2002, "Numerical and Experimental Modeling of Pollutant Dispersion in a Street Canyon", *J. of Wind Engineering and Industrial Aerodynamics*, Vol 90, pp.321-339.
- Sini, J.F., Anquetin, S. and Mestayer, P.G., 1996, "Pollutant dispersion and thermal effects in urban street canyons", *Atmospheric Environment*, Vol. 30, pp. 2659-2677.
- Tsai, M.Y., Chen, K.S and Wu, C.H., 2005, "Three-dimensional Modeling Dispersion in an Urban Street of Air Flow and Pollutant Canyon with Thermal Effects", *J. of the Air & Waste Manag. Association*, Vol. 55, pp. 1178-1189.
- Xie, X., Huang, Z., Wang, J. and Xie, Z., 2005b, "The Impact of Solar Radiation and Street Layout on Pollutant Dispersion in Street Canyon", *Building and Environment*, Vol. 40, pp. 201-212.
- Xie, X., Liu, C., Leung, D.Y.C., Leung, M.K.H., 2006, "Characteristics of Air Exchange in a Street Canyon with Ground Heating", *Atmospheric Environment*, Vol. 40, pp. 6396-6409.
- Xie, X., Liu, C. and Leung, D.Y.C., 2007, "Impact of Building Facades and Ground Heating on Wind Flow and Pollutant Transport in Street Canyons", *Atmospheric Environment*, Vol. 41, pp. 9030-9049.

7. RESPONSIBILITY NOTICE

The authors are the only responsible for the printed material included in this paper.